Resistive Wall Mode in a periodic cylinder

H. Strauss

11-15-21

This note compares simulations with the M3D-C1 code [1] of the resistive wall mode (RWM) and resistive wall tearing mode (RTWM). The RWM branches from a marginally stable external kink surrounded by an ideally conducting wall. The RTWM branches from a marginally stable tearing mode with an ideally conducting wall. A circular large aspect ratio geometry is assumed Fig.1. The model [2, 3] assumes a constant current density $j = 2/q_0$ for $r < r_0$. For $r > r_0$ $j = 0$ and

$$q = q_0 \left(\frac{r}{r_0}\right)^2 . \tag{1}$$

The region $r > r_0$ is treated as a vacuum, except for the thin resistive wall at $r_w \le r \le r_w + \delta$, where δ is the wall width. The rational surface $q = q_s = m/n$ is at $r_s/r_0 = (q_s/q_0)^{1/2}$, in the vacuum region. The dispersion relation for a resistive wall mode (RWM) with a thin wall is [2, 3, 1]

$$\gamma\tau_{wall} = -m\frac{1-(m-nq_0)}{1-(m-nq_0)-(r_0/r_w)^{2m}} \tag{2}$$

where $\tau_{wall} = \mu_0\delta/(2\eta_{wall})$, $\tau_A = \sqrt{\mu_0\rho_0}R_0/B_0$, $q_0 = 2B_0/(R_0\mu_0 J_0)$. Simulations were done of a thin wall RWM model [1], as in Fig.1. The simulations are of a case with $r_0 = 0.8825a, r_w = 1.2a$, and $q_0 = 1.1$, where $a = 1$. Note that the rational surface r_s is in the inner vacuum region. It is useful to introduce the dimensionless wall Lundquist number $S_{wall} = \tau_{wall}/tau_A$. The growth rate is proportional to S_{wall}^{-1}.

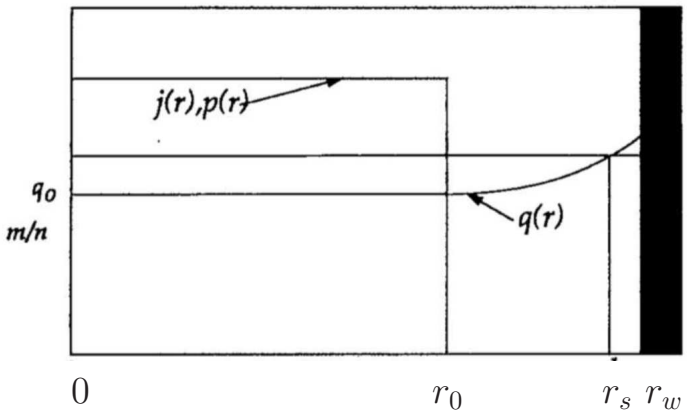

Figure 1: *Finn model equilibrium. The current is nonzero for* $0 \le r < r_0$. *The mode rational surface is at* $r = r_s$. *The wall is at* $r = r_w$. *The region* $r > r_w$ *is vacuum.*

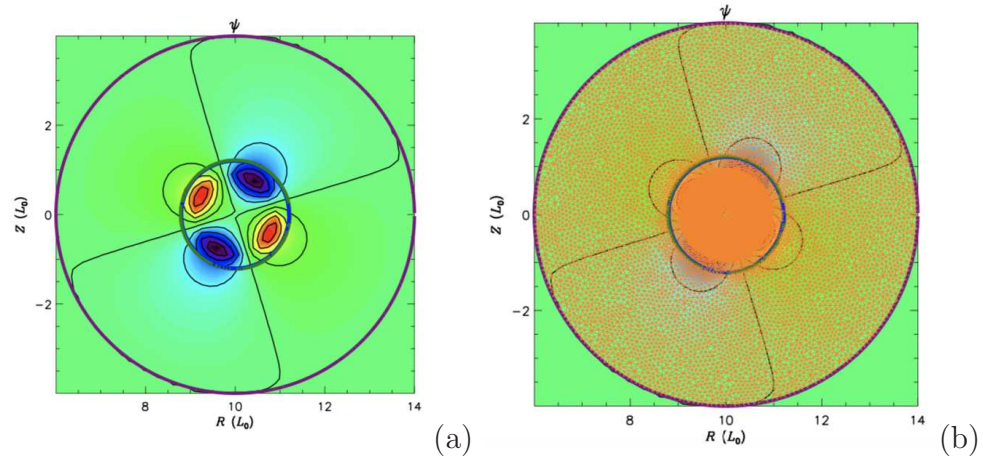

Figure 2: *(a) ψ with $S_{wall} = 10^4$. (b) mesh used for (a) The same mesh was used for all the runs in Fig.3. Apparently some mesh points around the wall are omitted.*

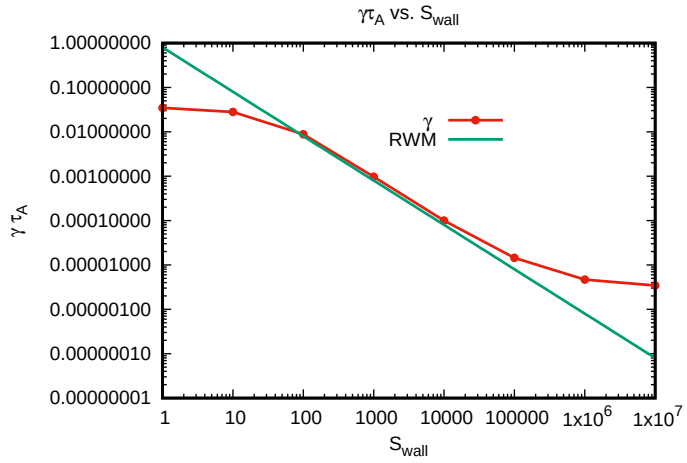

Figure 3: *γ vs. S_{wall} with thin wall. The fit is to a RWM $\propto S_{wall}^{-1}$.*

Reduced MHD was solved with the M3D-C1 code in a straight cylinder as in [1] and compared with the theory.

$$\frac{\partial \psi}{\partial t} = \mathbf{B} \cdot \nabla \phi + \eta \nabla^2 \psi \tag{3}$$

$$\frac{\partial \nabla^2 \phi}{\partial t} = \mathbf{B} \cdot \nabla \nabla^2 \psi \tag{4}$$

$$\mathbf{B} \cdot \nabla \phi = \nabla \psi \times \nabla \psi \cdot \hat{\zeta} + \frac{R_0}{R} \frac{\partial \phi}{\partial \zeta} \tag{5}$$

Fig.2(a) shows linear ψ for the case $S_{wall} = 10^4$. Fig.2(b) shows the adapted mesh used in all the cases. The mesh has a thin wall, $\delta = 0.02$. Fig.3 shows growth rate γ as a function of S_{wall}. For $S_{wall} \geq 10^5$, the most ustable mode appears to be a slightly unstable kink. The straight line fit is to S_{wall}^{-1} for a RWM.

The growth rate of a resistive wall tearing mode (RWTM) can be obtained from a limit of the dispersion relation obtained in [2]. The linear growth rate of the tearing mode (TM) [4] is given by

$$\gamma \tau_A = c_1 (\Delta' r_s)^{4/5} S^{-3/5} \tag{6}$$

$$c_1 = 0.55 \left(\frac{m q' r_s}{q^2} \right)^{2/5} \tag{7}$$

where r_s is the rational surface and m is the poloidal mode number. The model Fig.1 can be applied to the RWTM. Instead of vacuum outside the current channel, it is now assumed that the region $r < r_w$ is filled with resistive plasma, with a constant Lundquist number S. The rational surface r_s now is located in the plasma. At the wall $r = r_w$ [2]

$$\Delta'_w = \frac{2m}{r_s} \frac{nq_0 - (m-1) - (r_0/r_w)^{2m}}{[nq_0 - (m-1) - (r_0/r_s)^{2m}][1 - (r_s/r_w)^{2m}]} \tag{8}$$

If the wall is ideal, then the marginal stability condition for a tearing mode is $\Delta'_w = 0$ implies q_0 is

$$nq_0 = (m-1) + (r_0/r_w)^{2m}. \tag{9}$$

For $(m, n) = (2, 1)$, then $q_0 = 1 + (r_0/r_w)^4$. Combining (1), (9),

$$\frac{r_s}{r_0} = \left[\frac{2}{1 + (r_0/r_w)^4} \right]^{1/2} \tag{10}$$

The no wall Δ' is

$$\Delta'_\infty = -\frac{2m}{r_s} \frac{nq_0 - (m-1)}{nq_0 - (m-1) - (r_0/r_s)^{2m}},$$

which is Δ'_w with $r_w \to \infty$. Using the condition (9) gives

$$\Delta'_\infty = \frac{2m}{r_s}\frac{1}{(r_w/r_s)^{2m}-1}. \tag{11}$$

It was shown in [2, 6]

$$\Delta' = \frac{\hat{R}\Delta'_w + \Delta'_\infty}{1+\hat{R}}$$

where the quantity $\hat{R}$ is defined

$$\hat{R} = \frac{\gamma\tau_{wall}}{2m}[1-(r_s/r_w)^{2m}]$$

Assuming $\hat{R} \gg 1$ and $\Delta'_w = 0$ the dispersion relation was obtained in [6],

$$\gamma\tau_A = \frac{c_0}{S^{1/3}S_{wall}^{4/9}} \tag{12}$$

where

$$c_0 = 2.46\left(\frac{q'r_s}{q^2}\right)^{2/9} f^{4/9} = 2.46 f^{4/9} \tag{13}$$

$$f = \frac{(r_s/r_w)^{2m}}{[1-(r_s/r_w)^{2m}]^2} \tag{14}$$

The quantity $\hat{R}$ is

$$\hat{R} = \frac{c_0 S_w^{5/9}}{4S^{1/3}}\left[1-\left(\frac{r_s}{r_w}\right)^4\right] \tag{15}$$

Simulations were done for a similar case to the RWM with $r_0 = 0.88a, r_w = 1.2a$. The constraint (9) is $q_0 = 1.2925$. The rational surface is at $r_s = 1.098a$, then $r_s = 1.098a$. Then $\gamma\tau_A = 3.89S^{-1/3}S_{wall}^{4/9}$, and $\hat{R} = 0.29S_w^{5/9}S^{-1/3}$.

If $\hat{R} \ll 1$, then the dispersion relation is (6) with $\Delta' = \Delta'_\infty$, a no wall tearing mode.

Simulation results are shown in Fig.4. The dependence of γ on S_{wall} with $S = 10^4$, is shown in Fig.4(a). Both $\gamma\tau_A$ and a fit to $S_{wall}^{-4/9}$ are plotted. The fit is good for $S_wall \geq 10^6$. The dependence of γ on S, with $S_{wall} = 10^6$, is plotted in Fig.4(b). Here the fit to $S^{1/3}$ is surpringly good for low S.

This note reports on linear simulations of the RWM and RWTM with M3D-C1. It is expected to extend this work by taking rotation into account, and carry out nonlinear simulations. Similar linear and nonlinear simulations for realistic magnetic fusion experiments should be performed.

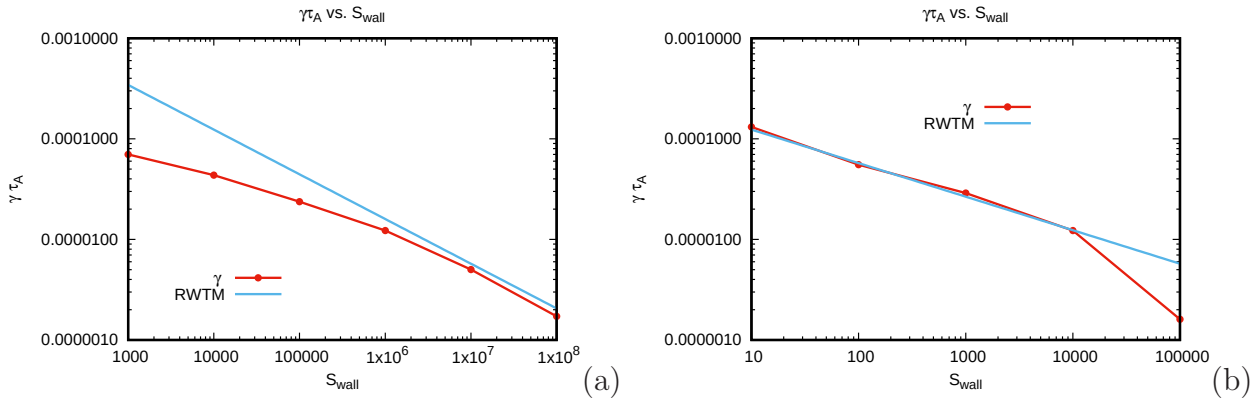

Figure 4: *(a)* $\gamma(S_{wall})$ *for case with* $q_0 = 1.295$, $\eta = 10^{-4}$. *The asymptotic fit is to* $S_{wall}^{-4/9}$. *(b)* $\gamma(\eta)$ *for same case but* $S_{wall} = 10^6$. *The fit is to* $S^{-1/3}$.

References

[1] N. M. Ferraro, S. C. Jardin, L. L. Lao, M. S. Shephard, and F. Zhang, Multi-region approach to free-boundary three-dimensional tokamak equilibria and resistive wall instabilities, Phys. Plasmas 23, 056114 (2016); https://doi.org/10.1063/1.4948722

[2] John A. Finn, Stabilization of ideal plasma resistive wall modes in cylindrical geometry: the effect of resistive layers, Phys. Plasmas 2, 3782 (1995)

[3] Fabio Villone, Yueqiang Liu, Guglielmo Rubinacci and Salvatore Ventre, Effects of thick blanket modules on the resistive wall modes stability in ITER, Nucl. Fusion 50 (2010) 125011.

[4] H. P. Furth, P. H. Rutherford, and H. Selberg, Phys. Fluids **16**, 1054 (1973)

[5] H. Strauss and JET Contributors, Effect of Resistive Wall on Thermal Quench in JET Disruptions, Phys. Plasmas **28**, 032501 (2021); doi: 10.1063/5.0038592.

[6] H. Strauss and JET Contributors, Effect of Resistive Wall on Thermal Quench in JET Disruptions, Phys. Plasmas **28**, 032501 (2021); doi: 10.1063/5.0038592.